Experimental Evidence for Pore Blocking as the Mechanism for Nitrogen Sorption Hysteresis in a Mesoporous Material

Sean P. Rigby*,† and Robin S. Fletcher‡

Department of Chemical Engineering, University of Bath, Claverton Down, Bath BA2 7AY, U.K., and Johnson Matthey Catalysts, P.O. Box 1, Belasis Avenue, Billingham, Cleveland TS23 1LB, U.K.

Received: November 17, 2003

The theory of "pore blocking" is often used, particularly in combination with percolation theory, to develop methods of analysis for gas sorption data for the structural characterization of porous media. However, the evidence for the existence of the pore-blocking effect is conflicting and equivocal. In the work described here mercury porosimetry experiments were integrated with gas sorption to detect the existence of pore-blocking effects during the desorption of nitrogen from a mesoporous sol−gel silica material at 77 K.

Introduction

Under certain sets of conditions, in the capillary condensation region of a type IV gas sorption isotherm, there are often two different values of relative pressure corresponding to the same amount of gas adsorbed, depending on whether the adsorption or desorption branch is considered. This hysteresis occurs in the capillary condensation region of the sorption isotherms for a range of different adsorbate−adsorbent pairs. Its particular cause in each case often remains unknown. Cohan[1] suggested that hysteresis might arise for pores consisting of cylinders open at both ends because of the difference in the shapes of the menisci during adsorption and desorption. Prior to adsorption the meniscus is cylindrical in shape, while prior to desorption the meniscus is hemispherical. However, most real materials, such as mesoporous sol−gel silica or alumina catalyst supports, have more complex pore structures consisting of interconnecting networks of pore bonds or of voids and necks. The idea of "pore blocking" as an explanation for the hysteresis was introduced in the work of Kraemer[2] and McBain.[3] The pore-blocking theory suggests that desorption of the condensed liquid from a pore network is a cooperative process. The evaporation of the condensed liquid from a large pore is delayed if access to the vapor phase can be achieved only via a smaller adjacent pore. The archetypal example of this type of system is the so-called "ink-bottle pore". Extensive reviews of the ink-bottle/network effect in capillary condensation hysteresis have been made by Everett[4] and Gregg and Sing.[5] The idea of pore blocking has been used, in conjunction with percolation theory, by various workers, including Wall and Brown,[6] Mason,[7] Neimark,[8] and Seaton,[9] to estimate various characteristic parameters of a porous solid, such as pore connectivity, from nitrogen sorption isotherms.

Gas desorption and mercury intrusion have both been considered to be invasion percolation processes.[10] An effect, known as "pore shadowing" or "pore shielding", which has some similarity to pore blocking, also arises in mercury intrusion porosimetry.[11] Hence, if the pore-blocking effect is occurring, then the pore size distribution from gas desorption ought to match that obtained from mercury intrusion porosimetry.[10] Therefore, an apparently simple test for pore-blocking effects is to compare the pore size distributions obtained from both mercury intrusion and gas desorption.[10] However, this test is not as easy to perform as it might first appear. This is because the correct values of the constants (contact angle and surface tension) in the relationship (generally known as the Washburn equation) between the size of a pore and the pressure required to fill it are often unknown and, frequently, values are simply assumed. However, in recent work,[12] semiempirical alternatives to the Washburn equation have been obtained from calibrated expressions for the constants in the Washburn equation, obtained by Kloubek.[13] The calibration was achieved by measuring the particular pressure at which mercury entered each of a set of model porous solids, which each possessed regular pores with a uniform size that was already known from independent microscopy methods,[14] but where the pore size differed between different test materials. Using the calibrated Washburn equation, it was shown[15] that the pore size distributions obtained from mercury intrusion matched those obtained from nitrogen desorption for a range of different mesoporous alumina materials. These findings support the existence of pore-blocking effects in nitrogen desorption from mesoporous alumina.

In-situ small-angle neutron scattering (SANS) has been used[16] to confirm the general picture of gas adsorption within larger mesopores that consists of multilayer buildup followed by capillary condensation, according to the Kelvin equation. The SANS studies[16] supported the assumption that, in contrast to desorption, capillary condensation is governed by the structural properties of the single pores and is less affected by the network morphology. Light scattering studies[17,18] have been made of the adsorption and desorption of hexane in porous Vycor glass. Since the pores in empty Vycor are very small (∼5 nm), the material appears homogeneous on length scales comparable with the wavelength of light, and thus scatters light very weakly. On filling the void space with hexane during adsorption, the measured transmission of light was roughly independent of the pressure. When the pores are completely saturated with fluid, there is virtually no mismatch in the index of refraction, and the scattering is reduced even further. However, during desorption, the transmission exhibited a very sharp and narrow dip due to the strong scattering of light occurring at hexane pressures

* Corresponding author. Telephone: +44 (0)1225 384978. Fax: +44 (0)1225 385713. E-mail: S.P.Rigby@bath.ac.uk.
† University of Bath.
‡ Johnson Matthey Catalysts.

10.1021/jp031253s CCC: $27.50
Published on Web 03/19/2004

corresponding to the steep step decline in the desorption isotherm. During desorption, as the Vycor drains, only some pores are emptied at first. At this stage, all of the surrounding pores are still filled with fluid and are thus index matched to the glass, and hence they do not contribute to the scattering. There is thus a large scattering contrast between the regions of empty pores and the remaining Vycor, where the pores are still full. The difference in the degree of scattering, between adsorption and desorption, was attributed to the development of large-scale inhomogeneities in the spatial distribution of empty pores which were comparable in size with the wavelength of light and, thus, could cause an increase in scattering. These correlations were found to have a fractal dimension of 2.6, which is very near the value of 2.5 predicted for an invasion percolation process in a 3D pore-bond network.

Similar long-range correlations in the spatial distribution of the adsorbed liquid phase, during the desorption branch of the hysteresis loop, have been observed, using SAXS, in studies of the sorption of CH_2Br_2 in Vycor porous glass.[19,20] Kikkinides et al.[21] have used lattice gas model simulations of the sorption process in statistical reconstructions of Vycor glass to determine whether the experimentally observed spatial correlations of adsorbed liquid-phase arose because of the pore-blocking effect or from some other mechanism. Their simulations suggested that in certain regions of the pore space a behavior analogous to pore blocking is observed, while cavitation of the larger cavities takes place at different regions of the pore space (i.e. large pores empty despite the nonexistence of contact with the bulk vapor phase). The latter result was in line with recent findings of Sarkisov and Monson[22] obtained from molecular dynamics simulations. Their simulations showed an absence of pore-blocking effects in a simple ink-bottle-pore model. On desorption, the large cavity remained filled with liquid until pressures that were lower relative to those where filling occurred on adsorption. However, the evaporation of the fluid from the large cavity took place while the smaller neck remained filled with fluid. Hence, the simulated desorption isotherm for the ink-bottle-pore model contained two steps. It has also been suggested[23] that the results of a grand canonical Monte Carlo (GCMC) study of argon adsorption/condensation in mesoporous silica glass do not support the existence of pore blocking. Recently, an analysis, performed by Ravikovitch and Neimark,[24] of the hysteresis loops and scanning loops for adsorption within FDU-1 with ~15 nm spherical pores has suggested three mechanisms of evaporation from ink-bottle type pores. Depending on the adsorptive, the temperature and the size of adjacent pore necks, evaporation from a pore body can (i) be controlled by pore-blocking effects, or (ii) occur spontaneously due to the cavitation of the stretched metastable liquid, or (iii) occur by near-equilibrium evaporation in the region of hysteresis from unblocked cavities that have access to the vapor phase. The experimental data were found to agree with results from nonlocal density functional theory (NLDFT)[25] and Monte Carlo[26] simulations for capillary condensation in spherical cavities.

A recent study[27] that aimed at reproducing the sorption isotherms for water on Vycor glass at room temperature, using the concept of pore blocking together with the Kelvin equation, did not give rise to a realistic adsorption/desorption curve. A NMR study[28] of the adsorption/desorption hysteresis for water sorption in silica gels with pore sizes of ~10 nm showed that, at equivalent water saturation levels, there was no difference between the NMR relaxation times and self-diffusion coefficients for the condensed liquid phase obtained along the adsorption branch and those on the desorption branch. This finding suggested that the geometry and connectivity of the liquid phase was statistically the same along the two branches. Since, if pore-blocking effects were occurring during desorption, there should be differences in the geometry and topology of the condensed liquid phase between the two branches of the hysteresis loop, then these results suggest that pore-blocking effects were not occurring in this system.

TABLE 1: Parameters for Insertion into Equation 2 for Silica and Alumina Materials and Their Ranges of Validity

material	$A \times 10^3$/ ($N \cdot m^{-1}$)	$B \times 10^{12}$/ N	range of validity/nm
silica (advancing meniscus)	−302.533	−0.739	6−99.75
silica (retreating meniscus)	−68.366	−235.561	4−68.5
alumina (advancing meniscus)	−302.533	−0.739	6−99.75
alumina (retreating meniscus)	−40	−240	4−68.5

The above discussion of previous work suggests that the evidence for the existence of a pore-blocking effect during gas desorption is conflicting. It is the purpose of the work reported here to establish a test to directly determine whether the pore-blocking effect is occurring in a given adsorbent−adsorbate system. Integrated gas sorption and mercury porosimetry experiments[29,30] will be used to detect the presence of the pore-blocking effect occurring during the desorption of nitrogen from a sol−gel silica material. Rather than using a structured, mesoporous solid,[24] such as a SBA-type material, this work employs a more irregular, amorphous material. This is because irregular materials may exhibit behavior different from the more regularly structured porous solids. Analysis methods based on pore-blocking theory are often used to structurally characterize these irregular materials, and thus it is necessary to know whether these characterization methods are genuinely applicable to the materials to which they are applied.

In the integrated method[29,30] a set of gas sorption and mercury porosimetry experiments are run in series on the same sample. This is achieved by freezing in place the mercury that becomes entrapped within the void space following porosimetry before a subsequent gas sorption experiment is performed. In this work, a material with a pore structure analogous to an ink-bottle pore will be used. From a comparison of the desorption isotherms obtained both before and after the largest pores present in the material have been filled with frozen mercury, it is possible to deconvolve the particular desorption behavior exhibited by liquid nitrogen occupying these largest pores while there is a simultaneously condensed phase in the surrounding smaller pores.

Theory

In general, raw data from mercury porosimetry is analyzed using the Washburn[31] equation:

$$r = -\frac{2\gamma \cos\theta}{p} \tag{1}$$

where p is the applied pressure, r is the pore radius, γ is the surface tension, and θ is the contact angle. It is frequently assumed that both γ and θ are constants. However, it is well-known[32] that both the surface tension and contact angle vary with the radius of curvature of the meniscus and that the contact angle depends on whether the meniscus is advancing or receding. As mentioned above, more recently[13,30,33] correlations for the product $\gamma \cos\theta$ have been introduced that take into account these effects. As described above, the correlations are empirical in origin[13,14] and are, therefore, of limited range of applicability (see Table 1) and also contain experimental error (~4−5% [13]). However, the applicability of the correlations to

various silica and alumina materials has been independently validated using integrated gas sorption and mercury porosimetry experiments.[29,30] The general equation that results from using the empirical correlations[13,30,33] for $\gamma \cos \theta$ in eq 1 is given by

$$r = \frac{-A + \sqrt{(A^2 - 2pB)}}{p} \tag{2}$$

where the values of the constants A and B depend on the material under testing and whether the mercury meniscus is advancing or retreating. The values of A and B for silica and alumina are given in Table 1. Equation 2 can be used to deconvolve contact angle hysteresis from the contribution made by structural hysteresis.

The material used in this work is a sol−gel silica material denoted G1. Previous studies[12,29,34,35] have shown that the pore structure of this material consists of isolated, macroscopic domains of larger pores that are completely surrounded by a continuous network of smaller pores. This particular type of pore structure is analogous to the simple ink-bottle-pore model, as access to the largest pores present in the material is possible only via smaller pores. Hence, the material G1 is a good model for testing of the pore-blocking theory. G1 has a modal pore size of ∼10 nm. This pore size is similar to that of the silica gel material that was the subject of previous NMR studies[28] of water sorption.

This section briefly describes the range of experimental evidence that shows that pellets from batch G1 have the particular type of pore structure described above. For more details on the experimental methods employed and the interpretations made, the reader is referred to the appropriate references. Previous magnetic resonance imaging (MRI) studies[34] of whole pellet samples from batch G1 have shown that they possess nonrandom, macroscopic heterogeneities (0.01−1 mm) in the spatial distribution of local average pore size. When the raw data from mercury intrusion and extrusion curves for whole pellet samples taken from batch G1 were analyzed[12] using eq 2, it was found that hysteresis and entrapment is limited to only the largest pore sizes present in the material. When the raw mercury intrusion and extrusion curves for fragmented samples from batch G1, with particle sizes ∼30 μm, were analyzed[12] using eq 2 no hysteresis or entrapment was observed. In addition, a shift in the initial part of the intrusion curve to larger pore sizes was also observed[12] following fragmentation. These findings were interpreted[12] in the light of mercury porosimetry experiments conducted on glass micromodels by Wardlaw and McKellar.[36] These workers found that no mercury entrapment occurred at all in glass micromodels that consisted of networks of pores which all had very similar sizes. Wardlaw and McKellar[36] also produced models etched in glass that consisted of pore networks that possessed isolated regions, containing only larger pore elements, which were completely surrounded by a continuous network of smaller pore elements. In these models, mercury only entered the network when the pressure was sufficient to invade the smaller pore elements and then it completely filled the network. The continuous network of smaller pores "shielded" the regions of larger pores from the invading mercury. However, as the pressure was reduced, mercury withdrew initially only from the smaller pore elements. When the pressure was reduced to a level sufficient to empty the larger pores, these had already become isolated from contact with the edge of the model by snap-off of the mercury menisci, and extensive residual mercury was retained. The work of Wardlaw and McKellar[36] suggested that, for whole pellets from batch G1, mercury becomes entrapped within isolated, spatially extensive regions that only contain larger pores but which are themselves surrounded by a continuous sea of smaller pores which gives rise to the pore-shielding effect that in turn causes the entrapment. Since the pore-shielding effect, giving rise to the mercury entrapment, is removed when the pellets are fragmented to particles of ∼30 μm size, then the regions of larger pores must be of this order in size or larger. Since pellets from batch G1 are transparent to visible light, light microscopy studies of pellets are possible both before and after porosimetry. Light microscopy studies[35] have confirmed that the spatial distribution of entrapped mercury within whole pellets from batch G1 is highly heterogeneous, whereas MR spin density images of fresh pellets have shown that the total porosity is relatively more evenly distributed. Entrapped mercury was found to occur in macroscopic domains of ∼0.1−1 mm size that were surrounded by clear regions containing no entrapped mercury at all. It was also found[35] that the level of mercury entrapment within whole pellets from batch G1 was independent of the equilibration time chosen for the porosimetry experiments, even for values up to 3600 s, and the macroscopic ganglia of entrapped mercury observed within pellets from batch G1 retained their particular morphology and location for several days following the experiment. These findings[35] suggested that entrapped mercury did not move during the course of the porosimetry experiment itself, or thereafter, and therefore apparent entrapment of mercury did not arise because of the longer migration distance necessary for disconnected mercury ganglia to reach the surface of whole pellets, compared to that of powder fragments.

Experimental Section

Samples for the experiments each consisted of a small number of sol−gel silica catalyst support pellets (of nominal 3 mm diameter) taken from a batch denoted G1. Nitrogen sorption experiments were carried out at 77 K using a Micromeritics ASAP 2400 apparatus. The sample tube and its contents were loaded into the degassing port of the apparatus and initially degassed at room temperature until a vacuum of 0.27 Pa was recorded. A heating mantle was then applied to the sample tube, and the contents were heated, under vacuum, to a temperature of 623 K. The sample was then left under vacuum for 14 h at a pressure of 0.27 Pa. The purpose of the thermal pretreatment for each particular sample was to drive off any physisorbed water on the sample but to leave the morphology of the sample itself unchanged. A range of different thermal pretreatment procedures has been considered in the past[12] in order to determine whether the experimental results were sensitive to the temperature or time period used. For all samples, at this point the heating mantle was removed and the sample allowed to cool to room temperature. The sample tube and its contents were then reweighed to obtain the dry weight of the sample before being transferred to the analysis port for the automated analysis procedure. The sample was then immersed in liquid nitrogen at 77 K before the sorption measurements were taken.

Following the first nitrogen sorption experiment, the sample was allowed to reach room temperature (298.9 K) and then transferred to the mercury porosimeter still under nitrogen. Mercury porosimetry experiments were performed using a Micromeritics Autopore IV 9420. The sample was first evacuated to a pressure of 6.7 Pa in order to remove physisorbed gases from the interior of the sample. The standard equilibration time used in the experiments was 15 s. Since it is difficult to thoroughly clean entrapped mercury from a given sample after

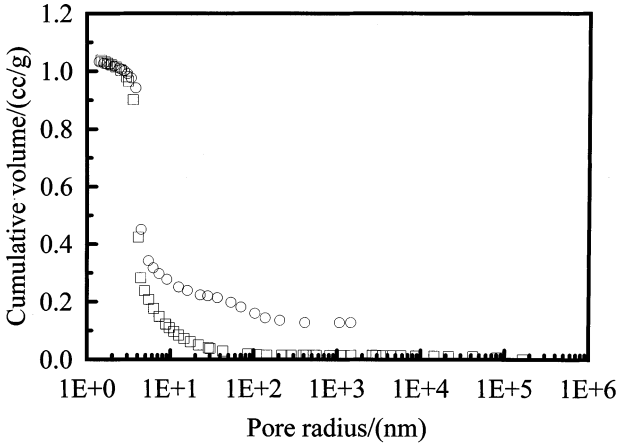

Figure 1. Mercury porosimetry intrusion (□) and retraction (○) curves, analyzed using eq 2, for a whole pellet sample from batch G1 (where "1E+2", for example, represents 1×10^2).

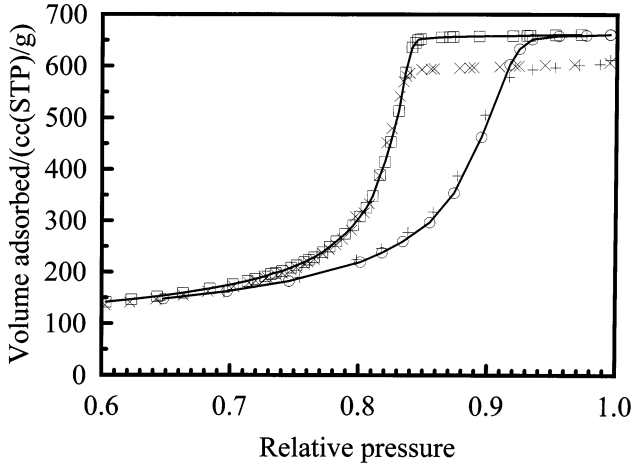

Figure 2. Superposition of the hysteresis loop regions of the nitrogen sorption isotherms obtained both before and after mercury porosimetry for a whole-pellet sample from batch G1. (Before porosimetry: adsorption (○); desorption (□). After porosimetry: adsorption (+); desorption (×)). The equilibration time used in the experiments was 5 s. The lines shown are to guide the eye.

an experiment for reuse in a further mercury porosimetry experiment, each particular set of experiments was, instead, repeated on several samples from the same batch. Following mercury porosimetry the sample was transferred back to the nitrogen sorption apparatus. The sample was then cooled to 77 K to freeze the mercury in place. Following the cooling of the sample, it was evacuated to vacuum and the next nitrogen sorption experiment commenced.

Results and Discussion

Integrated nitrogen sorption and mercury porosimetry experiments were conducted on several whole pellet samples taken from batch G1. These experiments consisted of an initial gas sorption run, followed by mercury porosimetry, and, subsequently, a final gas sorption run. In one series of experiments the equilibration time used in the gas sorption experiments was 5 s, whereas in a second set of experiments the equilibration time was 50 s. Figure 1 shows the data obtained from the mercury porosimetry experiments that have been analyzed using eq 2 and the constants from Table 1 appropriate to silica materials. From Figure 1, it can be seen that, within the error present in eq 2, the intrusion and extrusion curves are superimposed at smaller pore sizes and that the hysteresis and entrapment of mercury only occurs at larger pore sizes.

Figure 2 shows a superposition of the hysteresis regions of the nitrogen sorption isotherms obtained both before and after a mercury porosimetry experiment. The data in Figure 2 were obtained using an equilibration time of 5 s. From Figure 2 it can be seen that both the adsorption and the desorption isotherms obtained after mercury porosimetry are identical, within experimental error, to those obtained before mercury entrapment for amounts adsorbed below ~600 cm^3(STP)/g. However, it can also be seen that the position of the final flat plateaus in the adsorption isotherms has decreased in value from ~660 to ~600 cm^3(STP)/g following mercury entrapment. In the adsorption experiment conducted before mercury entrapment, additional nitrogen continued to be adsorbed at relative pressures above the value where the adsorption isotherm obtained after porosimetry had already flattened off to the point where subsequent adsorption was negligible. A *t*-plot analysis of the nitrogen adsorption isotherms obtained before and after mercury entrapment showed that there was no increase in micropore volume following mercury entrapment and freezing. This result confirms that the thermal contraction of mercury during cooling to 77 K does not create microporous cracks big enough for nitrogen to penetrate. The above findings are consistent with the proposal that the entrapped mercury only occupies the largest pores in the sample and then completely prevents adsorption of nitrogen into these pores.

From Figure 2 it can be seen that, for relative pressures between the values of ~0.92 and ~0.85, the desorption isotherms obtained both before and after mercury entrapment are exactly parallel to each other. The desorption isotherm obtained after mercury entrapment separately shows the relative pressures at which desorption commences from the smaller pores that originally shielded the largest pores (that have since become filled with entrapped mercury). The difference between the desorption isotherms obtained before and after mercury entrapment shows the desorption behavior of the condensed phase in the largest pores. From Figure 2, it can be seen that, when free of mercury, desorption from the largest pores only commences when desorption from the surrounding smaller pores has also commenced at a relative pressure of <~0.85. This finding suggests that the presence of condensed nitrogen within the surrounding smaller pores does prevent desorption of condensed nitrogen from the shielded largest pores. Since, in a disordered material, one small pore can block access to many larger pores, then the amount of the condensed phase desorbed from the larger pores can be much greater than the amount desorbed from the blocking smaller pore at the same relative pressure. Hence, the desorption isotherm obtained before mercury entrapment is steeper than the desorption isotherm obtained after porosimetry in the range of relative pressures between ~0.85 and ~0.84, where desorption in the latter isotherm commences. In the isotherm obtained before mercury entrapment, the section of the desorption branch corresponding to the largest pores (amounts adsorbed > ~600 cm^3 (STP)/g) is steeper than the section of the adsorption branch corresponding to the same pores. This is consistent with what would be expected if smaller pores are blocking access to the largest pores.

It is conceivable that the delay in the desorption from the largest pores, which are surrounded by smaller pores, may arise due to mass-transfer limitations. Figure 3 shows a superposition of the hysteresis regions of the nitrogen sorption isotherms obtained both before and after a mercury porosimetry experiment on another whole-pellet sample taken from batch G1. However, the data in Figure 3 were obtained using an equilibration time

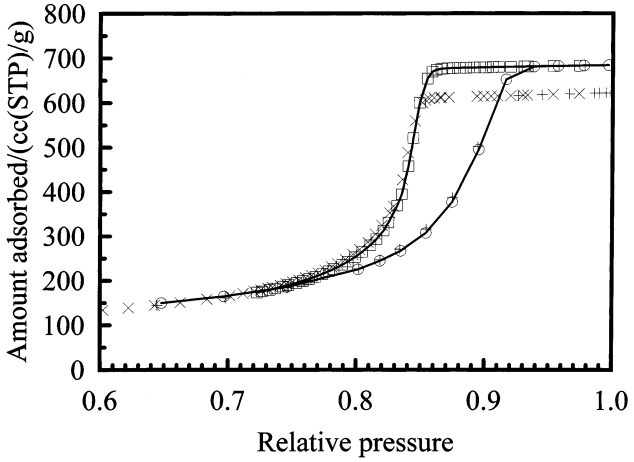

Figure 3. Superposition of the hysteresis loop regions of the nitrogen sorption isotherms obtained both before and after mercury porosimetry for a whole-pellet sample from batch G1. (Before porosimetry: adsorption (○); desorption (□). After porosimetry: adsorption (+); desorption (×)). The equilibration time used in the experiments was 50 s. The lines shown are to guide the eye.

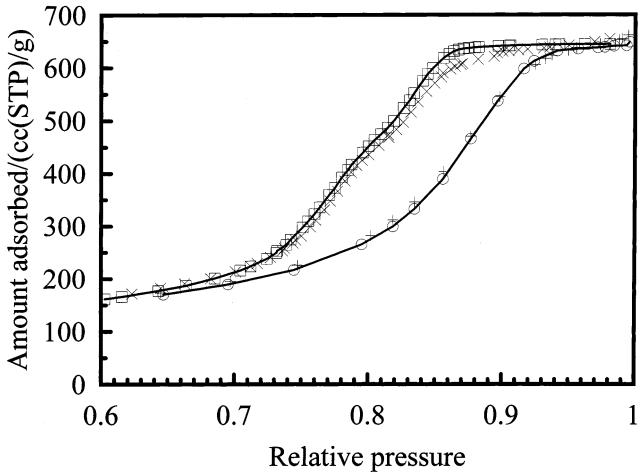

Figure 4. Superposition of the hysteresis loop regions of the nitrogen sorption isotherms obtained both before and after the fragmentation of a sample of whole pellets from batch G1. (Before fragmentation: adsorption (○); desorption (□). After fragmentation: adsorption (+); desorption (×)). The lines shown are to guide the eye.

of 50 s, rather than 5 s as in Figure 2. The longer equilibration time provides a longer time period in which the nitrogen molecules can diffuse out of the sample. Hence, if a slow mass-transfer rate were causing the apparent blocking effect, then that effect would be expected to be diminished when a longer diffusion time is allowed. However, allowing for minor intra-batch variability, it can be seen that the shapes of the respective isotherms in Figures 2 and 3 are identical. Hence, it seems unlikely that slow mass transfer is giving rise to the apparent pore-blocking effect in this case.

An additional set of nitrogen sorption experiments was performed on a further sample taken from batch G1. In these experiments gas sorption isotherms were initially obtained for the whole-pellet sample. After the first gas sorption run, the whole pellets were fragmented to form a powder with particle sizes of $\sim$100 μm. The typical particle size is still $\sim 10^4$ times larger than the typical pore size in G1. The sample was then degassed, and a further set of gas sorption isotherms was obtained. In previous work,[12] it has been shown that the internal surface of pellets from batch G1 does not undergo any reconstruction following repeated degassing procedures according to the method described above. The BET surface areas derived from the adsorption isotherms obtained before and after the fragmentation of the whole pellets were 333 ± 1 and 340 ± 1 m^2 g^{-1}, respectively. The small increase in total surface area, following fragmentation, can be attributed to the creation of additional external surface area of the particles due to size reduction. Hence the BET results suggest that the fragmentation process has not damaged the internal pore structure of the pellets, since the internal surface area accessible to nitrogen has not changed significantly. Figure 4 shows the superposition of the hysteresis loop region of the sorption isotherms obtained before and after fragmentation of the whole pellets from batch G1. It can be seen that, within experimental error, the adsorption isotherms are identical to each other. However, it can also be seen that the hysteresis loop has narrowed following fragmentation of the pellets. In particular, it can be seen from Figure 4 that the top section of the hysteresis loop (at amounts adsorbed $> \sim$600 cm^3(STP)/g) has narrowed markedly following fragmentation. This result suggests that when many of the surrounding smaller pores are removed by the fragmentation of the pellet, much of the condensed nitrogen within the largest pores can then desorb at higher relative pressures than it could for whole pellets. The fragmentation of pellets possessing macroscopic heterogeneity in the spatial distribution of pore size allows the "neck" of the "ink bottle" to be removed. Hence, the pore-blocking effect is removed, and desorption from the largest pores can occur at higher relative pressures.

The above results suggest that the smaller pores surrounding the largest pores in whole pellets from batch G1 cause a delay in the desorption of condensed nitrogen to lower relative pressures, but that this delay can be removed by fragmentation of the pellets. From the work of Sarkisov and Monson,[22] if the pore blocking effect was not operating in the desorption of condensed nitrogen from the largest pores in whole pellets from batch G1, then an additional step-down in the desorption isotherms in Figures 2 and 3, obtained for whole pellets before porosimetry, might be expected in the relative pressure range from $\sim$0.92 to $\sim$0.85. Since this additional step-down in the amount adsorbed does not occur, in Figures 2 and 3, and it is clear from Figure 4 that nitrogen would desorb from the largest pores in the sample in this range of relative pressures in the absence of the encircling smaller pores, then it is likely that the pore-blocking effect is taking place. Hence, the results reported here suggest that while pore-blocking may not occur for water desorption from similar silica materials with a similar pore size, as shown by NMR,[28] it does occur for nitrogen desorption from the particular silica gel material studied here. Ravikovitch and Neimark[24] have suggested that pore blocking only takes place when the pore-neck diameter exceeds a characteristic size, which is $\sim$4 nm for nitrogen. Since eq 2 suggests that a typical mercury porosimeter, capable of reaching pressures up to $\sim$414 MPa ($\sim$60 000 psi), can intrude pores of diameters down to $\sim$3 nm, then the integrated gas sorption and mercury porosimetry method might also potentially investigate the mechanism of hysteresis in materials with pore necks of $\sim$4 nm size. This will be the subject of a future work.

Conclusions

Previous work has shown that the pore structure of pellets from batch G1 is analogous to the so-called "ink-bottle-pore" model. The integrated gas sorption and mercury porosimetry experiments have shown that desorption of condensed nitrogen from the largest pores present in whole pellets from batch G1

is delayed until desorption commences from smaller pores in the sample. Nitrogen sorption experiments on fragmented samples from batch G1 have shown that desorption from the largest pores present in the sample can commence at higher relative pressures than in the whole pellet if the surrounding smaller pores are removed. These findings have suggested the operation of a "pore-blocking" effect in the desorption of condensed nitrogen at 77 K from the largest pores in whole pellet samples from batch G1.

References and Notes

(1) Cohan, L. H. *J. Am. Chem. Soc.* **1938**, *60*, 433.

(2) Kraemer, E. O. In *Treatise on Physical Chemistry*; Taylor, H. S., Ed.; Van Nostrand: New York, 1931; p 1661.

(3) McBain, J. W. *J. Am. Chem. Soc.* **1935**, *57*, 699.

(4) Everett, D. H. In *The Solid−Gas Interface*; Flood, E. A., Ed.; Dekker: New York, 1967; Vol. 2.

(5) Gregg, S. J.; Sing, K. S. W. *Adsorption, Surface Area and Porosity*; Academic Press: New York, 1982.

(6) Wall, G. C.; Brown, R. J. C. *J. Colloid Interface Sci.* **1981**, *82*, 141.

(7) Mason, G. *J. Colloid Interface Sci.* **1982**, *88*, 36.

(8) Neimark, A. V. *Stud. Surf. Sci. Catal.* **1991**, *62*, 67.

(9) Seaton, N. A. *Chem. Eng. Sci.* **1991**, *46*, 1895.

(10) Murray, K. L.; Seaton, N. A.; Day, M. A. *Langmuir* **1999**, *15*, 8155.

(11) Androutsopoulos, G. P.; Mann, R. *Chem. Eng. Sci.* **1979**, *34*, 1203.

(12) Rigby, S. P.; Edler, K. J. *J. Colloid Interface Sci.* **2002**, *250*, 175.

(13) Kloubek, J. *Powder Technol.* **1981**, *29*, 63.

(14) Liabastre, A. A.; Orr, C. *J. Colloid Interface Sci.* **1978**, *64*, 1.

(15) Rigby, S. P.; Barwick, D.; Fletcher, R. S.; Riley, S. N. *Appl. Catal., A* **2003**, *238*, 303.

(16) Smarsly, B.; Goltner, C.; Antonietti, M.; Ruland, W.; Hoinkis, E. *J. Phys. Chem. B* **2001**, *105*, 831.

(17) Page, J. H.; Liu, J.; Abeles, B.; Deckman, H. W.; Weitz, D. A. *Phys. Rev. Lett.* **1993**, *71*, 1216.

(18) Page, J. H.; Liu, J.; Abeles, B.; Herbolzheimer, E.; Deckman, H. W.; Weitz, D. A. *Phys. Rev. E* **1995**, *52*, 2763.

(19) Kikkinides, E. S.; Kainourgiakis, M. E.; Stefanopoulos, K.; Mitropoulos, A. Ch.; Stubos, A. K.; Kanellopoulos, N. K. *J. Chem. Phys.* **2000**, *112*, 9881.

(20) Mitropoulos, A. Ch.; Haynes, J. M.; Richardson, R. M.; Kanellopoulos, N. K. *Phys. Rev. B* **1995**, *52*, 10035.

(21) Kikkinides, E. S.; Kainourgiakis, M. E.; Stubos, A. K. *Langmuir* **2003**, *19*, 3338.

(22) Sarkisov, L.; Monson, P. A. *Langmuir* **2001**, *17*, 7600.

(23) Pellenq, R. J. M.; Rousseau, B.; Levitz, P. E. *Phys. Chem. Chem. Phys.* **2001**, *3*, 1207.

(24) Ravikovitch, P. I.; Neimark, A. V. *Langmuir* **2002**, *18*, 9830.

(25) Ravikovitch, P. I.; Neimark, A. V. *Langmuir* **2002**, *18*, 1550.

(26) Vishnyakov, A.; Neimark, A. V. *Langmuir* **2003**, *19*, 3240.

(27) Bentz, D. P.; Garbocci, E. J.; Quenard, D. A. *Mol. Simul. Mater. Sci.* **1998**, *6*, 211.

(28) Porion, P.; Faugere, A. M.; Levitz, P.; Van Damme, H.; Raoof, A.; Guilbaud, J. P.; Chevoir, F. *Magn. Reson. Imaging* **1998**, *16*, 679.

(29) Rigby, S. P.; Fletcher, R. S.; Riley, S. N. *Chem. Eng. Sci.* **2004**, *59*, 41.

(30) Rigby, S. P.; Fletcher, R. S. submitted for publication in *Part. Part. Syst. Charact.*

(31) Washburn, E. W. *Phys. Rev.* **1921**, *17*, 273.

(32) Van Brakel, J.; Modry, S.; Svata, M. *Powder Technol.* **1981**, *29*, 1.

(33) Rigby, S. P. *Stud. Surf. Sci. Catal.* **2002**, *144*, 185.

(34) Rigby, S. P.; Gladden, L. F. *Chem. Eng. Sci.* **1996**, *51*, 2263.

(35) Rigby, S. P.; Fletcher, R. S.; Riley, S. N. *Appl. Catal., A* **2003**, *247*, 27.

(36) Wardlaw, N. C.: McKellar, M. *Powder Technol.* **1981**, *29* 127.